



# Stemflow infiltration hotspots near-tree stems along a soil depth gradient in a mixed oak–beech forest

Ondřej Hemr<sup>1</sup> · Tomáš Vichta<sup>2</sup> · Martina Brychtová<sup>1</sup> · Petr Kupec<sup>1</sup> · Nikola Žižlavská<sup>3</sup> · Gabriela Tomášová<sup>2</sup> · Jan Deutscher<sup>1</sup>

Received: 30 March 2023 / Revised: 16 June 2023 / Accepted: 29 June 2023 / Published online: 24 July 2023  
© The Author(s) 2023

## Abstract

In an upland forested micro-catchment during the growing season, we tested soil responses to precipitation events as well as soil water content (SWC). We asked ourselves if what is the difference of SWC response to precipitation events depending on the presence and proximity of a tree? The environmental heterogeneity of the small 7.5-ha headwater area was captured by soil probes at specific locations: (i) probe measurements of SWC at 10-, 30-, 60-, and 100-cm depths; (ii) resolution of near-tree (NT) and between-tree (BT) positions; and (iii) resolution of four slope classes. The results revealed significant differences between the hydrological responses of the soil. NT soils had faster infiltration but were also faster to dry out when compared to BT soils, which were less affected by the presence of trees. Water input threshold values, measured as the precipitation amount needed to cause a significant increase in SWC, were also significantly different, with NT positions always lower than BT positions. Total infiltration of the topmost NT and BT soil layers reached 185 and 156 mm during the study period, corresponding to 43% and 36% of the total 434 mm of precipitation, respectively. Infiltration into the deepest horizon was significantly higher in NT soils, where it reached 114 mm (26%) as opposed to 9 mm (2%) in BT soils, and was indicative of significant vertical hydraulic bypass flow in the proximity of trees. These observations contribute to better understanding the hydrological processes, their nonlinearity, and the expansion of conceptual hydrological models.

**Keywords** Soil water content · Watershed · Soil moisture dynamics · Slope class · Time-domain transmission methods · Growing season

## Introduction

The basic influence of vegetation on runoff (water yield) from forested catchments has been well documented after decades of research (Bosch and Hewlett 1982; Hrachowitz

et al. 2013), including the conditions in Central Europe (Eisenbies et al. 2007, Bíba et al. 2010, Švihla et al. 2016, Černohous et al. 2017). In general, reducing forest cover results in increased runoff, whereas reforestation reduces runoff in long term. Increased runoff has been attributed directly to the intensity of the reduction in forest cover (Patric 1978). At the same time, the hydrological response of a watershed to changes in vegetation cover is difficult to predict (Ganatsios et al. 2010).

The role of forests in mitigating floods (peak flows) is also significant; through evapotranspiration, trees create a deficit of soil moisture, which creates space for water retention. Among forest vegetation types, there are seasonal differences in water use and interception owing to phenological changes in the assimilation apparatus, which are mainly evident between evergreen and deciduous forests (Crockford and Richardson 2000; Eisenbies et al. 2007; Deutscher et al. 2016; Kupec et al. 2019). Also, different strategies in the root architecture can be observed especially between oak and

Communicated by Agustin Merino.

✉ Martina Brychtová  
martina.brychtova@mendelu.cz

<sup>1</sup> Department of Landscape Management, Faculty of Forestry and Wood Technology, Mendel University in Brno, Zemědělská 3, 613 00 Brno, Czech Republic

<sup>2</sup> Department of Geology and Pedology, Faculty of Forestry and Wood Technology, Mendel University in Brno, Zemědělská 3, 613 00 Brno, Czech Republic

<sup>3</sup> Department of Forest Management and Applied Geoinformatics, Faculty of Forestry and Wood Technology, Mendel University in Brno, Zemědělská 3, 613 00 Brno, Czech Republic

spruce forest strands; oak planting has a higher impact on soil hydraulic properties, i.e., soil structure recovery, higher soil infiltration rates, and capacity as well (Julich et al. 2021). Forest soils are generally associated with higher infiltration rates (Zimmermann et al. 2006; Agnese et al. 2011) and lower surface runoff (Jordán et al. 2008; Alaoui et al. 2011) than other land cover types. Tree roots increase the number of macropores in the soil, connect drainage paths, reduce soil compaction, and improve soil structure, thereby increasing the infiltration rate and soil water storage capacity (Malik et al. 2019; Guo et al. 2021; Revell et al. 2022). For a number of events, especially small- and medium-sized floods, additional forest can retain a considerable amount of water within the landscape, particularly in Central Europe, where river basins have been significantly altered in land-use structure (Wahren et al. 2012).

In this study, we deal with a smaller scale than a whole catchment. The study site is located in an elementary drainage area in the uppermost part of a forested upland headwater micro-watershed in the temperate part of Central Europe. Uplands are a common type of georelief in Central Europe, and their importance in water resource management is well recognized. Despite several comprehensive researches (McGlynn et al. 2002; Šamonil et al. 2010; Kuentz et al. 2017; McMillan 2020), we lack a sufficiently described influence of forest stands on the hydraulics of the soil environment, especially at the microscale. Understanding the role of trees in water retention and water availability in streams is important, especially during this period of rapid global warming.

The manner in which precipitation water reaches the soil in forest stands has been well described in the literature (Levia et al. 2017; Van Stan et al. 2020). The water input through the canopy is routed via stemflow and throughfall. Throughfall is precipitation that passes either directly through the canopy or is initially caught by aboveground vegetative surfaces and subsequently drips down to the forest floor. Stemflow is precipitation that flows from leaves and branches and is channeled to the plant stem (Levia et al. 2011). Interception is the precipitation retained by the canopy. During the growing season (leafy phase) in Central Europe, throughfall in beech (*Fagus sylvatica*) stands reaches approximately 65%, stemflow is 5%, and interception is 30% (Staelens et al. 2008; Frischbier et al. 2019). For a mixed forest with a predominance of beech and oak (*Quercus petraea*), throughfall reaches 76.3%, stemflow is 2.6%, and interception is 21.2% (Novosadová et al. 2023). Throughfall and stemflow values can vary significantly for different rainfall intensities. A study from Belgium showed that the amount of throughfall in the growing season does not exceed 12%, and stemflow does not exceed 8% for rainfall events of up to 5 mm (Staelens et al. 2006).

Both stemflow and throughfall reach the forest floor, where infiltration processes can begin. During infiltration, water enters the soil environment through the soil surface (Lal and Shukla 2004). The redistribution of infiltrated water is significantly affected by preferential flow pathways (Sidle et al. 2001), with multiple well-described flow pathways discerned as preferential. Early studies identified the importance of subsurface flow as a component of storm-period streamflow (Mosley 1979, 1982). Subsurface preferential flow is distinguished as laterally oriented *pipe flow* and rather vertically developed *macropore flow* (Jones 1971; Beven and Germann 1982, 2013; Uchida et al. 2001). There is a basic agreement that soil macropores originate from desiccation, growth, and decay of roots, mycelia, and burrowing animals (Coppola et al. 2009; Bachmair and Weiler 2011).

The infiltration area for stemflow near a tree is usually reported to be very small,  $< 1 \text{ m}^2$  (Carlyle-Moses et al. 2020). The infiltration area for beech has also been reported to be  $< 0.1 \text{ m}^2$  (Llorens et al. 2022) but can vary greatly from 0.04 to 11.8  $\text{m}^2$  (Herwitz 1986; Van Stan and Allen 2020). Studies have examined the differences in the ability of soil to infiltrate water depending on the distance from a tree: A study from the UK showed that at distances of 10 cm and 200 cm, there was 75% higher infiltration in winter and 25% in summer for the distance closer to the tree (Revell et al. 2022). This study was conducted on clay soils, and it is probable that this phenomenon is more significant in more permeable soils. However, other studies have indicated that soils with a higher proportion of clay particles create better conditions for macropore formation (Jarvis 2007; Koestel et al. 2012). At the same time, Metzger et al. (2021) found that at the microscale, soils near-tree trunks have lower field water capacity and higher hydraulic conductivity, indicating high macroporosity through both living and dead roots. The vertical movement of water through macropores can accelerate its transport; otherwise, transport occurs by filtering water through the soil matrix at a rate that is several orders of magnitude slower (Johnson and Lehmann 2006; Liang et al. 2011; Spencer and van Meerveld 2016).

The ability of trees to influence soil permeability also depends on the tree species and the architecture of its roots, most notably its depth and horizontal extent (Pohl et al. 2011), which affect other relevant soil attributes such as soil porosity, proportion of organic matter, and biomass (Chen et al. 2013; Hirte et al. 2018). Concurrently, the root type also affects soil water transport. While the main anchoring tap roots affect vertical water transport, fine (fibrous) roots have a greater effect on permeability in the lateral direction (Mitchell et al. 1995; Perkons et al. 2014; Fan et al. 2016). The simultaneous effect of primary and secondary roots on infiltration rate is not sufficiently understood (Zhang et al. 2019).

Slope inclination is another controlling variable associated with infiltration. One effect of slopes is the lower occurrence of standing surface water (Liu et al. 2011). Infiltration rates also generally decrease with increasing slope (Fox et al. 1997). The topography is an important factor for infiltration, especially during precipitation events. However, the position of the slope and soil depth can be variable due to differences in vegetation cover, microtopography, and heterogeneity of soil texture. The relationships among slope topography, soil properties, vegetation, and seasonal soil moisture patterns appear to be very complex (Dymond et al. 2021). One hypothesis to explain the dynamics of soil moisture on slopes is the so-called *fill and spill* (Tromp-Van Meerveld and McDonnell 2006), which considers the influence of the microtopography of the impervious subsoil and emphasizes the way the hydrological connectivity in subsurface saturated zones occurs. Another relevant phenomenon of slopes is the uprooting dynamics of forest stands. Developed post-uprooting terrain morphology can cause a slowdown in water runoff, increase the spatial heterogeneity of soil, and increase water retention (Šamonil et al. 2010; Valtera and Schaetzl 2017).

Nevertheless, our understanding of how trees affect soil hydraulic properties at the microscale remains limited (Chandler et al. 2018). Several studies have examined the chemistry (Dhiedt et al. 2022) or differences in the dynamics of soil moisture under the tree and between the crowns, but they are either from a different environment (Breshears et al. 2009), take into account only one position of the slope (Dymond et al. 2021), do not take the slope into account (Abdallah et al. 2020), or perform measurements on only

one soil depth (Ray et al. 2019; Rita et al. 2021). Jačka et al. (2020) and Juříčka et al. (2022) also analyzed the soil moisture gradient on pit-mound microrelief slope. To the best of our knowledge, no studies have been conducted that describe the effect of precipitation on the dynamics of soil moisture depending simultaneously on: (i) the position near the tree and between trees, (ii) different slope positions, and (iii) different soil depths. The absence of such work has been recognized in the current studies (Jochheim et al. 2022).

The effects of individual trees and the position on the slope on water transport are not well understood. Therefore, we aimed to answer the following questions: (1) What differences (if any) exist in the response of the slope soil environment to precipitation events depending on the presence of a tree? and (2) How does the presence of a tree affect the reaction to precipitation events and water distribution in the soil profile on a slope?

## Materials and methods

### Study site

The study was conducted in a micro-watershed of a left side nameless tributary of the Žilůvecký Brook in Babice nad Svitavou, Brno, Czech Republic (49.2901189 N, 16.6747356 E) (Fig. 1). The study site was located in the headwater area of an upland forested catchment in the temperate zone of Central Europe. The micro-watershed covers 7.59 ha with an altitude ranging 325 to 370 m a. s. l. The long-term 30-year average annual air temperature and

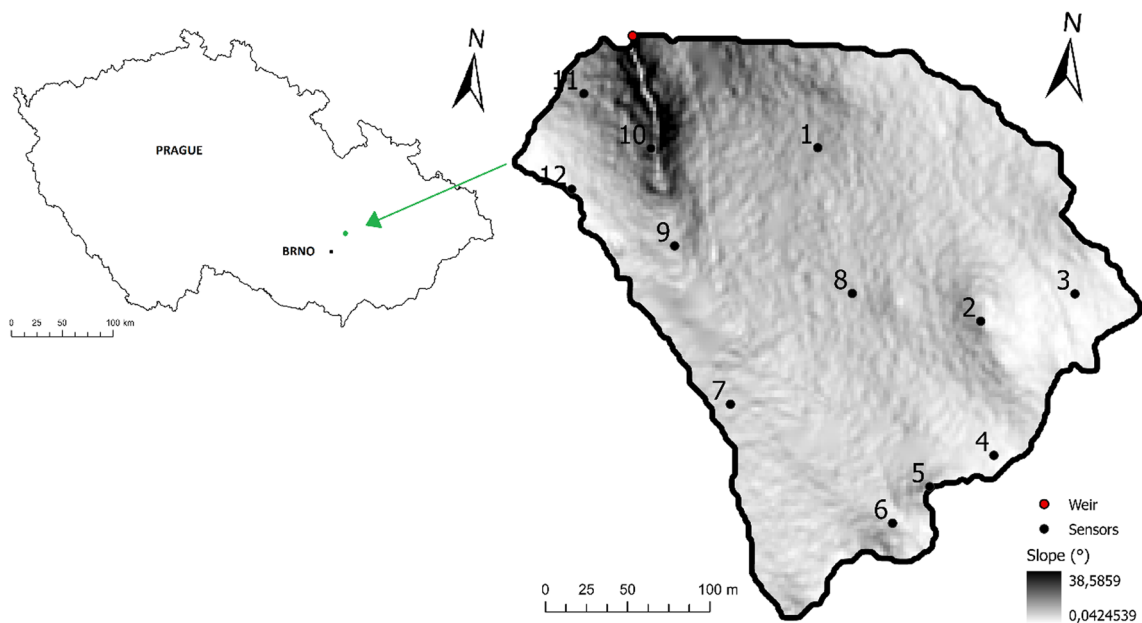


**Fig. 1** Study site (watershed) location within the Czech Republic (right), the watershed shape and its slope values (left)

the mean annual precipitation reach 10.0 °C and 606 mm, respectively, and April–October growing season 16.8 °C and 427 mm, respectively (CHMI 2023). For 2022, the seasonal values reached 14.8 °C and 434 mm, respectively.

Tree species composition on the site consists of sessile oak (*Quercus petraea* [Mat.] Liebl.), European beech (*Fagus sylvatica* L.), Scots pine (*Pinus sylvestris* L.), and European hornbeam (*Carpinus betulus* L.), with average proportions of 27.4, 28.5, 13.8, and 12.5%, respectively, along with an admixture of deciduous European larch (*Larix decidua* Mill.), Norway spruce (*Picea abies* (L.) H. Karst.), small-leaved lime (*Tilia cordata* Mill.), European ash (*Fraxinus excelsior* L.), and silver fir (*Abies alba* Mill.). Most of the stands comprise middle-aged trees of 61–81, 41–60, or 21–40 years, with a land cover of 45.5%, 32.7%, and 10.0%, respectively. Stands aged 1–20 years are rare, with an area of just 4.8%. The herbaceous undergrowth is typical of natural oak–hornbeam and beech–oak forests.

The subsoil consists of granodiorite with an irregular admixture of loess and loams, with actual soil type depending on loess loam thickness. Soils are classified as Hyper-skeletal Leptosols alternating with Skeletic Cambisols on upper slopes, Eutric (Haplic) Cambisols alternating with Gleyic Stagnosols on middle and lower slopes, depending on proximity to the stream source, and Skeletic Cambisols alternating with Luvic Cambisols on flats slope. Thus, the area displays a relatively high diversity of soil types, despite its relatively small size.

## Data acquisition

### SWC monitoring

Various electromagnetic methods based on the water–soil dielectric permittivity are typically used to measure the SWC of soils in situ (Vereecken et al. 2008). We used one of the most accurate time-domain transmission (TDT) methods (Robinson et al. 2003; Wild et al. 2019), which is suitable for ecological and hydrological catchment-scale observations. TDT sensors determine soil moisture more accurately than other methods because they do not register the trend of offset errors. Other types of sensors are burdened with this error, probably due to the limitations of the monitored soil sample volume and the effect of compaction around the electrodes during installation (Robinson et al. 2008). Initial calibration of the sensors was carried out in air under laboratory conditions. To prevent error due to the small measurement distance from the sensor, we installed each sensor in soil sieved through a 2-mm sieve. This type of sensor is usually installed in the vertical position; however, due to our measurement design, we proceeded to install them horizontally: (i) to better capture the areal distribution of roots, which are the transport interface for soil water flow, and (ii) to

capture spatial gradients between soil profiles, especially in the 10 cm = Ah/B horizons.

Time changes were monitored using the TMS-4 microclimate data logger (Wild et al. 2019), which continuously registers SWC using the TDT method discussed above. Each sensor was placed in a horizontal position in approximately 2-L pocket of purposely sieved soil (< 2 mm) to eliminate erroneous measurements caused by coarse rock fragments.

The study area was divided into four slope classes (Fig. 2) using ArcGIS Topographic Position Index tool (Weiss 2001). Three measuring nests were installed on each slope class. Two soil profiles were located in each measuring nest: (i) near-tree (NT), positioned downslope 50 cm from a tree trunk; and (ii) between-tree (BT), positioned downslope from a tree trunk in the nearest crown gap, which represented a location unaffected by stemflow. In each case, the SWC was measured under the tree species with similar root architecture, i.e., beech, oak, and hornbeam. The sensors were placed 10, 30, 60, and 100 cm below the surface. The depth of the soil did not reach 60 and 100 cm in all the positions, which resulted in different numbers of sensors at the individual depths (N). The following depths were available in each slope class: upper slope (UPPS): 10 and 30 cm; middle slope (MIDS) and flat slope (FLATS): 10, 30, and 60 cm; and lower slope (LOWS): 10, 30, 60, and 100 cm. This design resulted in 12 paired positions with measured soil profiles, and a total of 72 TMS-4 sensors were installed in the study area.

The map represents the elementary drainage area with identified slope classes and sensor locations: (a) upper

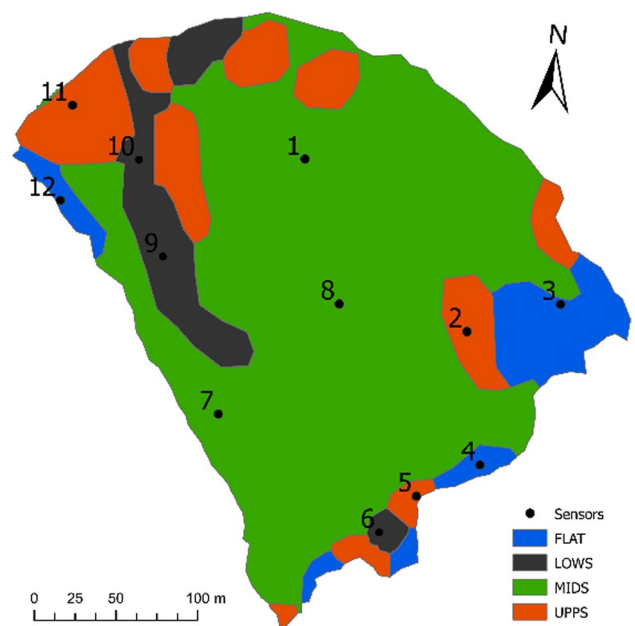


**Fig. 2** Spatial distribution of four slope classes. Slope information and sensor placement

slope locations (UPPS # 2, 5, and 11); (b) middle slope locations (MIDS # 1, 7, 8, and 3); (c) lower slope locations (LOWS # 6, 9, and 10), and (d) flat slope locations (FLATS # 3, 4, and 12).

The sensors were set up to obtain readings every 15 min. The sensors were installed at the site during September and October 2021; however, to ensure sufficient consolidation of the returned soil, monitoring began on April 1, 2022, at the beginning of the growing season. The sensor output was TMS Moisture Signal data “raw data,” which were later converted to SWC individually for each slope and depth position (see “SWC conversion” Section).

### Soil temperature and rainfall monitoring

The soil temperature was monitored using a TMS-4 sensor in the same measurement mode as the SWC. The soil temperature was used as a factor for the selection of precipitation periods to ensure that the ground was never frozen (see “Selection of infiltration events and their statistical evaluation” Section). Rainfall and air temperature were measured at 15-min intervals by a climatic station (AMET, Litschmann and Suchý, Velké Bílovice, Czech Republic) located approximately 0.5 km away from the study site.

## Data processing and statistical analysis

### SWC conversion

The TMS calibration utility (Wild et al. 2019) was used to convert “raw data” (~500–3600) to volumetric soil moisture (0–100%). Other input data used in the conversions include: (i) soil particle size distribution (PSD; clay: less than 0.002 mm; silt: 0.002–0.05 mm; and sand: 0.05–2 mm) and (ii) soil bulk density (BD), which defined the calibration curves. These two soil properties were determined based on soil samples collected individually from each sensor location ( $n=72$ ). The output of this conversion was a 72-soil moisture time series that reflected the specific PSD and BD for each slope class, NT/BT position, and depth. This conversion achieved the maximum possible level of quality for the detected SWC for subsequent analyses.

### 2.3.2. Summary statistics

The 15-min SWC records were aggregated into daily average values for each individual depth. These data are presented in Table 1. Data were tested for normality using the Shapiro–Wilk test. None of the series passed the normality test, so the non-parametric Wilcoxon test was used. Statistical analyses were performed using R software (R version R 4.2.1 GUI 1.79 High Sierra build and RStudio version 2022.07.2 + 576; R Core Team 2017).

**Table 1** Descriptive statistics of the SWC time series: (I) median SWC ( $\text{cm}^3/\text{cm}^3$ ); (II) mean SWC ( $\text{cm}^3/\text{cm}^3$ ); (III)  $N$ =number of sensors in a depth; (IV) mean SD=mean standard deviation calculated from daily SDs for every day in the period; (V) CV=coefficient of variation; (VI) DF of NT and BT=difference of mean SWC between NT and BT ( $\text{cm}^3/\text{cm}^3$ ); (VII) non-parametric Wilcoxon test; (VIII)

max SWC=maximum SWC ( $\text{cm}^3/\text{cm}^3$ ); (XI) min SWC=minimum SWC ( $\text{cm}^3/\text{cm}^3$ ); (X) RS to prec=response to precipitation calculated as the maximum inter-day increase in SWC ( $\text{cm}^3/\text{cm}^3$ ); (XI) ReS of RS=% response to precipitation to mean SWC; and (XII) DF of prec RS of NT to BT=% difference of relative precipitation response between NT and BT

Depth and location	10-cm NT	10-cm BT	30-cm NT	30-cm BT	60-cm NT	60-cm BT	100-cm NT	100-cm BT
Median SWC	0.300	0.306	0.271	0.274	0.303	0.314	0.357	0.323
Mean SWC	0.287	0.304	0.277	0.286	0.303	0.321	0.357	0.334
$N$	12	12	12	12	9	9	3	3
Mean SD	0.050	0.065	0.062	0.037	0.082	0.071	0.066	0.068
CV (–)	0.17	0.22	0.22	0.13	0.27	0.22	0.18	0.20
DF of NT and BT <sup>a</sup>	–0.016**		–0.008		–0.018***		0.023***	
WXP test <sup>a</sup>	0.0086		0.0761		8.76E–08		1.631E–15	
Max SWC	0.395	0.399	0.366	0.380	0.353	0.371	0.414	0.379
Min SWC	0.157	0.193	0.179	0.199	0.246	0.267	0.302	0.300
RS to prec	0.117	0.102	0.075	0.065	0.031	0.019	0.042	0.004
ReS of the RS	40.9	33.6	27.1	22.7	10.3	6.0	11.7	1.1%
DF of prec RS of NT to BT	7.3		4.4		4.3		10.5	

$p$ -value \*\* < 0.01, and \*\*\* < 0.001

<sup>a</sup>Wilcoxon test

## Selection of infiltration events and their statistical evaluation

The study period was the growing season, which lasted from April 1 to October 31, 2022. During this period, we attempted to identify all non-negligible infiltration events (Liang et al. 2011), regardless of the source rainfall characteristics (quantity/intensity). We used the procedure from Wang et al. (2013) and assumed that water reached a certain depth when the soil moisture content began to increase. The uppermost (10 cm) soil layer at the NT position was used as the representative soil layer. We selected time periods that met the following criteria for rainfall infiltration events (RIEs): (i) The soil temperature did not fall below 0 °C; (ii) SWC increased by more than 0.005 cm<sup>3</sup>/cm<sup>3</sup> (Liang et al. 2011) at a depth of 10 cm in the NT position; and (iii) the end of the event was set when the SWC reached a steady regime, following the method described by Wang et al. (2008).

For individual RIEs, minimum and maximum SWC values for each depth, slope class, and NT and BT positions were analyzed. Values greater than 0 indicated infiltration and negative values indicated zero soil response to the rainfall event. By adding  $\Delta$ SWC for all NT and BT positions at the respective depths, we obtained the total positive SWC change that occurred throughout the entire growing season in cm<sup>3</sup>/cm<sup>3</sup>, which corresponds to the total rainfall infiltration during the growing season. This relative volume change was recalculated as cumulative amounts in milliseconds of infiltrated water according to the depth of the horizon and its SWC. The two topmost sensors (10 cm and 30 cm) represent 20 cm of soil depth, i.e., 0–20 and 20–40 cm, respectively. The two deep sensors (60 cm and 100 cm) represent a soil depth of 40–80 and 80–120 cm, respectively. In total, up to 120 cm of soil depth was described this way.

The  $\Delta$ SWC series were tested for normality using the Shapiro–Wilk test. No series passed the test; therefore, the non-parametric Wilcoxon test was used to indicate the differences between  $\Delta$ SWC for NT and BT at each depth. The  $\Delta$ SWC series were then correlated to the sum of the precipitation in individual RIEs. Correlations with Pearson's correlation coefficient were graphically presented using the ggplot2 function in R ("ggplot2" package version 3.4.1; Wickham 2016).

## Results

### General trends in the dynamics of SWC

During the 2022 growing season, 19 RIEs and non-negligible infiltration events occurred (Fig. 3). The precipitation in the events ranged from 5.1 to 47.25 mm, and the rainfall

intensity ranged from 1.03 to 6.80 mm/h. Total precipitation during RIEs reached 315 mm out of 435 mm for the entire period, which corresponds to approximately 72% of all precipitation infiltrated in the topsoil NT. Therefore, 28% of total precipitation did not cause infiltration. Upon visual inspection, SWC in the NT and BT positions exhibited the following fundamental differences:

- (1) The decrease in SWC after the peak was always greater at the NT positions and at all depths. This is less apparent at the beginning and end of the growing season; we attribute this phenomenon to the ongoing evapotranspiration (ET) of trees.
- (2) The peak of the SWC increase was more pronounced in NT compared to BT. This phenomenon was more obvious when the total precipitation was higher and similar at all depths.
- (3) The difference in SWC dynamics was most noticeable at a depth of 100 cm. For BT, there were practically no changes in SWC and, therefore, no infiltration (or runoff) of rainwater in the deepest layers of the soil. Concurrently, for NT, there was a regular increase during RIEs, as well as a persistent decrease in SWC after the initial peak. This indicates that both infiltration and some form of water uptake occurred, suggesting different roles of the NT and BT positions in vertical hydrological connectivity.

Across all slope classes, the coefficient of variation for all the depths and for both NT and BT positions reached approximately 20% (13–27%; Table 1). This supports the mean SWC as a relevant descriptive characteristic for long-term (the duration of the growing season) evaluation and reflects the robustness of the experimental design. Even though there was variability in the data (see Table 1), this suggests that the long-term soil response can be interpreted regardless of the slope class position.

The mean SWC was approximately 1% (0.8–1.8%) higher in BT position than that in NT position in all but the deepest horizon. In the deepest horizon, the mean SWC was more than 2% higher in the NT position. This indicates that the largest amount of water was retained in the deepest horizon, NT. The maximum reaction to precipitation calculated from inter-day changes was higher in NT than that in BT at all depths and was approximately 11% in the deepest horizon, indicating higher infiltration in the NT positions.

### The soil reaction to precipitation during RIEs

The highest correlation of  $\Delta$ SWC to precipitation amounts was in the topmost layer (10-cm depth,  $n = 12$ ; Fig. 4) where  $R^2$  reached 0.76 and 0.70 for NT and BT, respectively. The  $b$  coefficient of the linear trend was interpreted as the

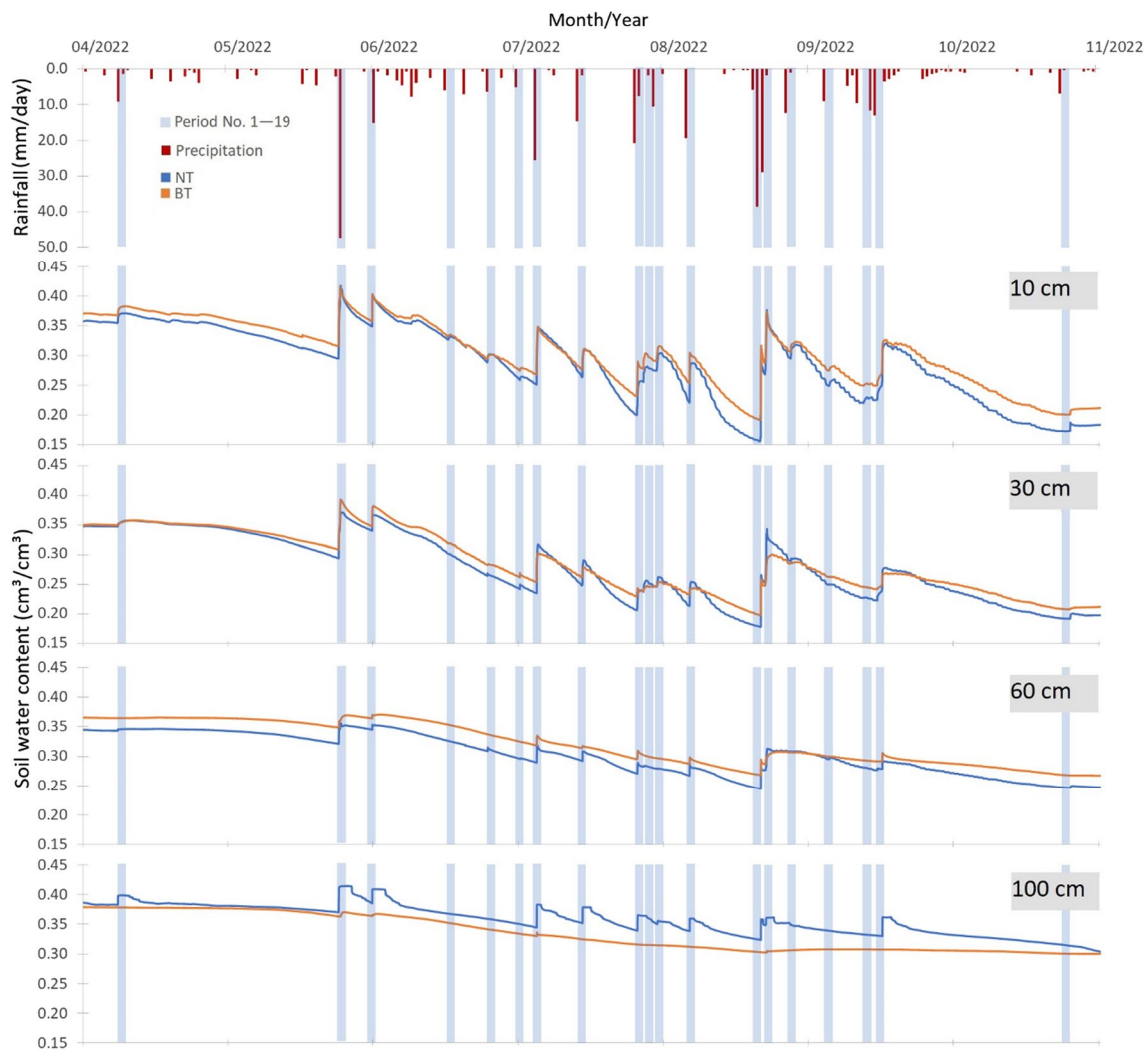


**Fig. 3** SWC dynamics in NT and BT positions during the 2022 growing season at depths of 10, 30, 60, and 100 cm. Dark blue line indicates average SWC for all NT positions at specific depths and orange

line likewise for BT positions. Light blue vertical strips indicate distinguished infiltration events and red lines on the very top indicate precipitation. (Color figure online)

threshold value for the water input (for infiltration to occur). In the topmost soil layer, it reached 5.48 and 6.68 mm for NT and BT, respectively. In addition, individual slope classes reacted slightly differently.

At depths of 30 cm ( $N=12$ ), a decrease in the correlation was evident (0.44 and 0.56 for NT and BT, respectively). As shown in Fig. 4, the two linear trend lines are wide apart, indicating a considerable difference in the reaction to precipitation, especially for higher precipitation events. The threshold for water input occurred at 10.6 and 10.3 mm for NT and BT, respectively; however, a significantly higher variability from 5 to 37 mm was observed. In addition, there were a number of events with precipitation amounts over 20 mm, causing very little infiltration.

At depths of 60 cm ( $N=9$ ), a further decrease in the correlation was evident (0.44 and 0.25 for NT and BT,

respectively). The linear trend lines of both NT and BT were almost parallel. The thresholds for water input were 11.3 and 14.0 mm for NT and BT, respectively. In some of the slope classes, the reaction to precipitation was negligible, especially for BT (red dots along the vertical axis; Fig. 4).

At depths of 100 cm ( $N=3$ ), the correlation was surprisingly high, especially for NT (0.66 and 0.37 for NT and BT, respectively). The two trend lines are wider apart, and NT exhibited a much higher infiltration. The threshold for water input was 7.2 and 12.8 mm for NT and BT, respectively. The differences in this deep soil layer were mainly caused by the extremely low reactivity of the BT positions. This indicates that in BT, most of the infiltration water did not reach the deepest soil layer, even in the case of several precipitations above 20 mm and one above 45 mm.

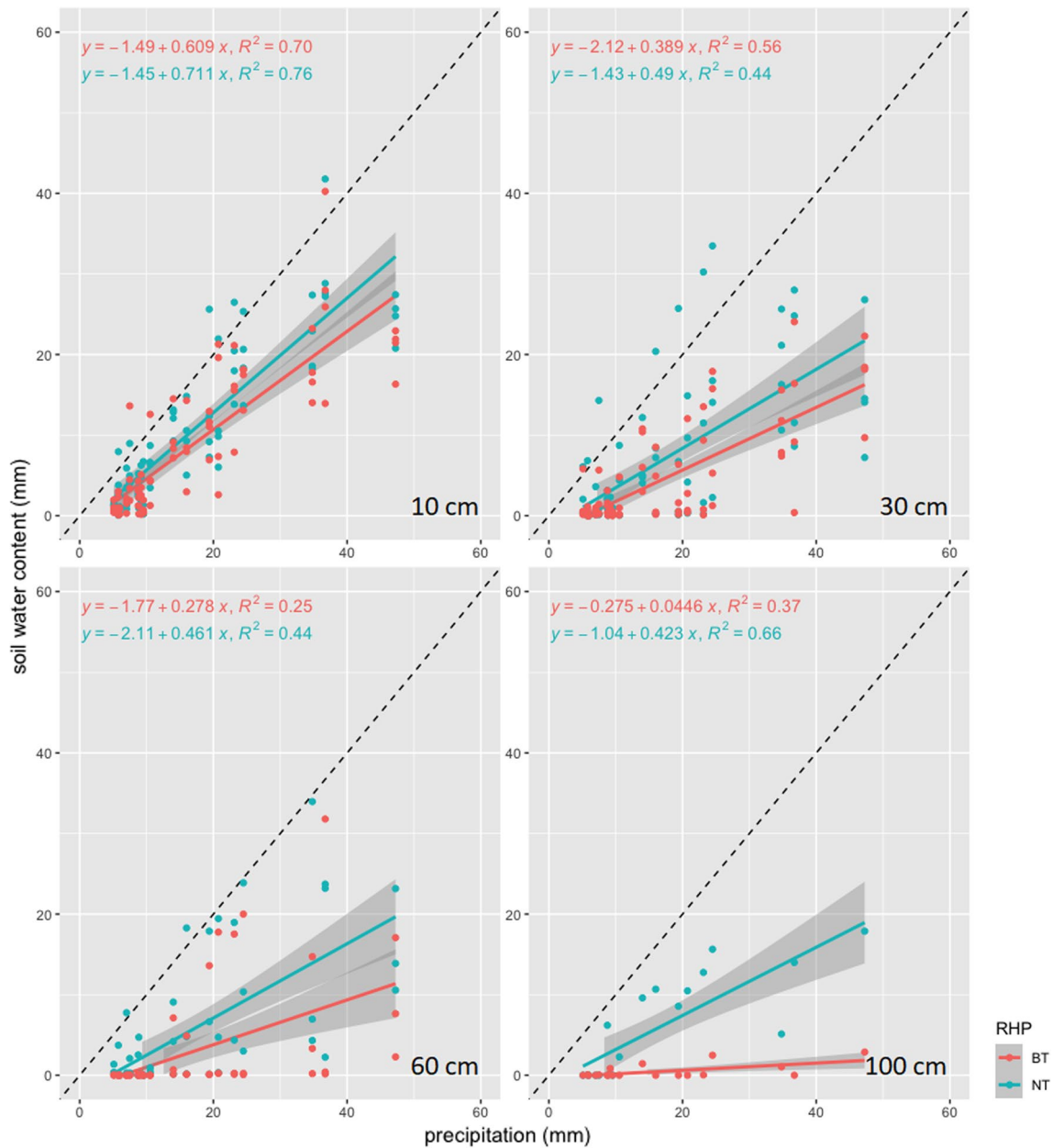


**Fig. 4** The correlation of  $\Delta$ SWC (mm) to the sum of precipitation during RIEs; BT=red. NT=blue (points and lines); the gray interval represents the confidence interval at the significance level  $p < 0.05$ ;

dashed line is 1:1 ratio of precipitation sum (mm) to  $\Delta$ SWC (mm). (Color figure online)

The three upper soil layers exhibited similar behavior in response to precipitation events. The greatest difference was observed in the deepest layer (100 cm). Notably, the water input threshold of NT was 5–6 mm lower than that of BT. At the same time, the unexpectedly high correlation in the NT horizon (higher in the upper layers at 30 and

60 cm) is indicative of good hydraulic connectivity and probably the so-called hydraulic bypass (see Discussion).

### Cumulative infiltration for the study period

Total infiltration reached 185 and 156 mm in the uppermost horizon at NT and BT, corresponding to 43% and

**Table 2** Cumulative water inputs for 10, 30, 60, and 100 cm during the 2022 growing season

	NT	BT	Difference	Ratio	Vertical decrease	
Cumulative water input (mm)	185.4	156.2	29.2	1.2	NT	BT
	121.0	76.2	44.7	1.6	64.40	79.94
	94.8	51.6	43.2	1.8	26.20	24.62
	113.6	8.8	104.8	12.9	–18.84	42.80
Ratio of water input (%)	43	36	7	1.2	NT	BT
	28	18	10	1.6	0.15	0.18
	22	12	10	1.8	0.06	0.06
	26	2	24	12.9	–0.04	0.10
Frequency of infiltration events (n)	19	16	3	1.2	NT	BT
	14	13	1	1.1	5	3
	10	8	2	1.3	4	5
	11	2	9	5.5	–1	6

36% of the total 434 mm of precipitation, respectively (Table 2). With increasing depth, it was possible to observe a decrease in the amount of infiltrated water, both absolutely and relatively (vertical decrease), except for the deepest soil layer (100 cm) in the NT position. Here, the infiltration was significantly higher in the NT position, where it reached 114 mm (26%) and only 9 mm (2%) in the BT position. The vertical connection between the 60- and 100-cm soil layers was very different for NT and BT. In the NT position, an increase of 4% was observed as opposed to a 10% decrease in the BT position. The fact that more water reached the deepest soil layer NT than the upper layer (60 cm) is indicative of some form of hydraulic bypass (see Discussion).

The ratio of water input was calculated as the proportion of cumulative water input at individual depths to the total precipitation during the study period. The values are arranged in descending order: 10, 30, 60, and 100 cm. In contrast with the long-term variability in the slope classes, which was rather low (Fig. 1), there was greater variability between the NT and BT positions for individual slope classes, which increased with soil depth (Table 3). At 10 cm, the variability was still very low (0.9–1.3), except for the LOWS class, where the ratio increased to 2.0 but was still insignificant. At 30 cm, the variability was higher (0.7–2.3), except for the LOWS class, where the ratio reached 4.0, with a statistically significant difference. In contrast, for MIDS and FLATS, the ratio remained similar, with a slight predominance of water input in the BT positions. At 60-cm BT, a surprisingly low water input was found in the MIDS and LOWS classes, reaching only 12.8 mm and 3.9 mm, respectively, as opposed to the much higher input NT (59 and 175 mm in MISA and LOWS, respectively). In particular, the statistically significant disproportion of water input at LOWS reached 44.4 mm. Another statistically insignificant difference is the almost

**Table 3** Soil water content change ( $\Delta$ ) at distinguished soil depths within each hillslope class at NT and BT

DSmax	NT (mm)	BT (mm)	NT/BT
<i>10 cm</i>			
UPSS	258.90	199.09	1.3
MIDS	159.32	182.77	0.9
LOWS	181.62	90.90	2.0
FLATS	185.25	180.43	1.0
All	185.45	155.34	1.2
<i>30 cm</i>			
UPSS	252.23	110.82	2.3*
MIDS	46.63	67.47	0.7
LOWS	101.51	25.36	4.0**
FLATS	107.38	124.86	0.9
All	121.20	76.16	1.6
<i>60 cm</i>			
MIDS	59.15	12.79	4.6*
LOWS	175.04	3.94	44.4***
FLATS	80.34	144.76	0.6
All	95.42	50.88	1.9***
<i>100 cm</i>			
LOWS	113.36	8.74	13.0**

The maximum amount of water that has been shown to infiltrate a given aquifer in response to a precipitation event. For long events, some of the infiltrated water may have been lost (evapotranspiration and various types of runoff). Wilcoxon test,  $p$ -value \* < 0.05, \*\* < 0.01, and \*\*\* < 0.001

double water input BT at FLAT. For the deepest soil layers (100 cm), a significant disproportion (also absolute) of the water input reached 13.0 in favor of NT.

## Discussion

### Stemflow, water input precipitation threshold, and infiltration hotspots

The NT probes were placed 0.5-m downslope from a tree trunk, which Metzger et al. (2021) suggested as the average critical distance of the tree-to-soil effect. Here, we assumed the full effect of the crown on interception. BT probes were placed in the nearest canopy gap along the contour line. Here, we assumed that crown interception was close to zero and the throughfall precipitation to be almost identical to that in the open area where precipitation was measured. Novosadová et al. (2023) found similar conditions in a beech–oak stand during the growing season, where the throughfall reached 76.3% and stemflow 2.6%. We, therefore, assumed that the amount of effective rainfall would be significant and at least 20% higher at the BT positions compared to that in the NT positions. According to our results, the soil response does not reflect this; the sum of  $\Delta$ SWC was almost always higher for the NT positions (Table 3), which agrees with the results of similar studies (Pressland 1976; Llorens et al. 2022). Similarly, the precipitation threshold for water input in the 10-cm horizon was also lower (5.48 mm) in NT position compared to that in the BT position (6.68 mm) (Fig. 4). These findings suggest that the partitioning of rainfall to infiltration is even greater in the NT position than that in our results.

This could be explained by a combination of (i) a higher rooting at the NT position presenting an increased number of preferential infiltration pathways and (ii) the effect of stemflow, which represents a concentrated point source of water entry. Some studies show that the contribution of stemflow to water intake (total recharge) can reach approximately 10–20% (Taniguchi et al. 1996), according to German studies (Meesenburg et al. 2009) 10–16%, and according to a European comparison 3–25% (Germer et al. 2012). These values are likely dependent on the intensity of rainfall events (Jochheim et al. 2022) rather than on the total annual precipitation (Berger et al. 2008). The role of stemflow was also evidenced in our study by the longer duration of the increase in  $\Delta$ SWC at the NT positions after rainfall (Fig. 3). Trees are known to efficiently adapt the distribution of their root system and displace pore water (Al Hagrey 2007). The course of SWC at NT versus BT could be then partly explained by the different suction potential of the absorbing roots in BT positions which could make the infiltration on this position even more difficult.

We understand these phenomena to be clear evidence of the existence of stemflow infiltration hotspots. However, it should also be noted that the results can be affected by the method of selecting precipitation events that entered into this analysis. We specifically chose all significant infiltration

events when  $\Delta$ SWC increased by more than  $0.005 \text{ cm}^3/\text{cm}^3$  in the topmost soil layer (Liang et al. 2011), with no regard to the source of rainfall event intensity. During the study period, 28% of precipitation (approximately 121 mm; usually events less than 5 mm) did not result in significant infiltration and was excluded from the analysis. Limited rewetting of the soil, water infiltration, and percolation can also be partly explained by soil repellency, which is higher the lower the previous soil saturation, especially in topmost layer (Greiffenhagen et al. 2006; Wessolek et al. 2008). This can be one of the reasons for the nonlinear response of SWC to some precipitation events.

One possible use of our results is in the inclusion in conceptual hydrological models, especially meso- and micro-scale, which are numerous and frequently used in current hydrological and environmental assessment studies (Liu et al. 2019). In lumped hydrological models, preferential water flow is generally ignored, similar to physically based models, although there is an overstatement that all drainage from the basin is preferential (Weiler 2017). This allows for the incorporation of the current knowledge on preferential flow. For example, combined stemflow quantification (infiltration height converted to crown area) and quantification of the resulting SWC increase at individual depths can be the basis for the calibration of a detailed hydrological model.

### Slope class and preferential flow pathways

At NT LOWS, the course of cumulative  $\Delta$ SWC at depths of 10, 30, and 60 cm reached 181.62, 101.51, and 175.04 mm, respectively. The higher water input (75%) at 60 cm, as opposed to 30 cm, is indicative of some form of bypass flow. At BT LOWS, a similar course of  $\Delta$ SWC was not observed, and the values decreased with depth, reaching 90.90, 25.34, and 3.94 mm for 10, 30, and 60 cm, respectively. A plausible explanation is again offered by vertical preferential infiltration or hydraulic bypass fueled by stemflow. Regardless of slope class, this NT behavior is supported by the almost identical threshold for water input into the 30- and 60-m depths that reached 10.6 and 11.3 mm, respectively (Fig. 4). Interestingly, we observed a similar less pronounced phenomenon at BT FLATS, where the course of the increase in  $\Delta$ SWC was 180.43, 124.86, and 144.76 mm for 10, 30, and 60 cm, respectively. This behavior cannot be explained by stemflow, but rather by some form of vertical bypass flow or the manifestation of lateral pipe flow, possibly due to the existence of an underground burrow hole (Uchida et al. 2001). Also, the decreasing correlation and widening of linear trend lines in Fig. 4 may be indicative of preferential flow pathways typical for forest soil environment but also increasing complexity with depth. For the sake of completeness, the design we used could not capture this complexity in detail, though it was ultimately not our goal.

Another significant difference between the NT and BT positions was the behavior in the deepest 100-cm soil layer. The cumulative  $\Delta$ SWC increased by 113.36 and 8.74 mm for NT and BT, respectively (Fig. 3, Table 3). The apparent, but unquantified, decreasing course of NT SWC at depths of 100 cm was steepest in the summer months, as opposed to a rather stable course at BT, indicating transpiration and/or lateral runoff even at NT positions. Finally, a significant decrease rather than an expected increase in precipitation threshold for water input between 60 and 100 cm from 11.3 to 7.21 mm at NT positions can be explained again by preferential flow with the following explanations: (i) transformation of stemflow along the root system into infiltration, (ii) utilization of vertical bypass flow, or (iii) their combination (Ghestem et al. 2011).

In the case of oak stands, tracing experiments explain the existence of direct vertical water transport by preferential flow along the main vertical tap root (Danjon et al. 1999). Around beech trees, the root network controls the entry of stemflow water and provides lateral redistribution of water through the soil matrix. Due to this effect, large parts of the soil matrix can be bypassed by rapid interflow downslope as suggested in the previous studies (Schwärzel et al. 2012). Simultaneously, a greater amount of organic matter at NT positions, which is a more suitable habitat for earthworms, increases the occurrence of preferential flow in the soil and supports infiltration (Devitt and Smith 2002; Jačka et al. 2021). Earthworms create their own paths (burrows) and connect the gaps between soil particles, thereby promoting water retention in the soil and percolation. In deeper soil horizons, more permanent vertical burrows can be created, and deep tree roots play an important role in the preferential transport of water into the deeper layers of the soil profile (Tomlin et al. 1995; Pitkänen and Nuutinen 1998). This may explain why we also found indications of hydraulic vertical bypass flow at some BT positions, even though they were only found in the FLATS class.

In contrast, vegetation can efficiently deplete water from deeper layers through evapotranspiration and thus has a dominant influence on the connection/disconnection of surface water and groundwater (Banks et al. 2011). This was mentioned above, where our results confirmed faster water depletion from the 100-cm depth at the NT positions. The influence of topography on the hydrological functioning of slope environments has been studied for a long time. However, there is a gap in the knowledge regarding the influence of vegetation on temporal and spatial relationships and soil moisture gradients, especially in forest ecosystems (Troch et al. 2009).

The relationship between slope and soil moisture is related to (micro)topography, soil texture, and vegetation type (Burt and Butcher 1985; Nyberg 1996; Tromp-Van Meerveld and McDonnell 2006). The differences between different slope classes in a watershed are complex (Francis et al. 1986). We had difficulties locating field data with which we could

compare our results. Results of Dymond et al. (2017), for example, showed that according to the slope gradient, LOWS should generally be wetter than MIDS and UPPS, which was also confirmed in our case for MIDS (backslope) but not for UPPS (summit), where we registered a higher SWC at all available depths (10 and 30 cm), even at BT positions. At MIDS, we did not have SWC measured at the 100-cm depth. For UPPS, depth was not measured at 60 cm due to the low depth to the parental bedrock. Our results indicate that the role of the slope class is less important for long-term SWC dynamics when both precipitation-free and precipitation-affected periods are included (Table 1). However, it can be significant in the soil moisture reaction directly after rainfall and rainfall infiltration, especially in LOWS (Table 3).

## Application in hydrological modeling

One possible use of our results is in the inclusion in conceptual hydrological models, especially meso- and micro-scale, which are numerous and frequently used in the current hydrological and environmental assessment studies (Liu et al. 2019). In lumped hydrological models, preferential water flow is generally ignored, similar to physically based models, although there is an overstatement that all drainage from the basin is preferential (Weiler 2017). This allows for the incorporation of the current knowledge on preferential flow. For example, combined stemflow quantification (infiltration height converted to crown area) and quantification of the resulting SWC increase at individual depths can be the basis for the calibration of a detailed hydrological model (Fig. 5).

## Conclusions

We conducted a comprehensive study to investigate the influence of tree proximity and slope class on the dynamics of SWC in a 0–100-cm depth gradient. Unlike most similar studies, we did not focus on the details of individual events;

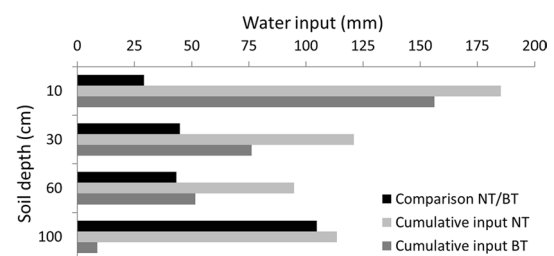


**Fig. 5** Cumulative water inputs for 10, 30, 60, and 100 cm during the 2022 growing season. Black color indicates the difference between NT and BT positions. Note the different behaviors in the deepest (100 cm) horizon where NT water input is even greater than the above (60 cm) horizon

rather, we tried to evaluate continuous SWC measurements in the context of the entire growing season to shed some light on the overall significance of the infiltration process in forested headwater areas. During the 2022 growing season, we demonstrated a distinctive difference in the SWC behavior based on the presence of a tree:

- (i) In close proximity (0.5 m) to trees (NT), SWC turned out to be more reactive to precipitation events, and this correlation was strongest in the topmost (10 cm) and deepest (100 cm) soil layers.
- (ii) In terms of the total precipitation, 41% and 35% infiltrated in the topmost layer, while 26% and 2% of precipitation infiltrated into the deepest layer at NT and BT locations, respectively, which was attributed to developed preferential flow and vertical hydraulic bypass in the proximity of trees.
- (iii) At the crown gaps (BT) in the deepest layer (100 cm), there was practically no reaction to precipitation events, even to extreme rainfall of up to 40 mm.
- (iv) In the transit zones (30 and 60 cm), a more complex hydraulic behavior was observed, which can be explained by the effects of transpiration, rooting density, and soil heterogeneity.
- (v) Despite an average lower SWC at NT for the entire season, NT positions demonstrated a higher hydroau-

lic connectivity and ability to infiltrate water into the deepest layers across all slope classes, despite approximately 20% higher effective precipitation totals at BT positions due to no canopy interception.

- (vi) The role of slope class was less important for long-term soil moisture dynamics. However, it proved to be very significant in the response to rainfall events and rainfall infiltration, especially in LOWS class.

Our study would contribute to the understanding of the effects of tree proximity and slope classes on soil moisture behavior in the environment of a predominantly broadleaved temperate forest stand. We believe that it can contribute to the understanding of hydrological processes, their nonlinearity, and the expansion of conceptual hydrological models. For future research, we plan to focus on the effect of specific tree species on near-stem infiltration and the effect of the winter season and snowmelt on the replenishment of soil moisture, depending on the distance from the tree.

## Appendix 1

See Fig. 6.

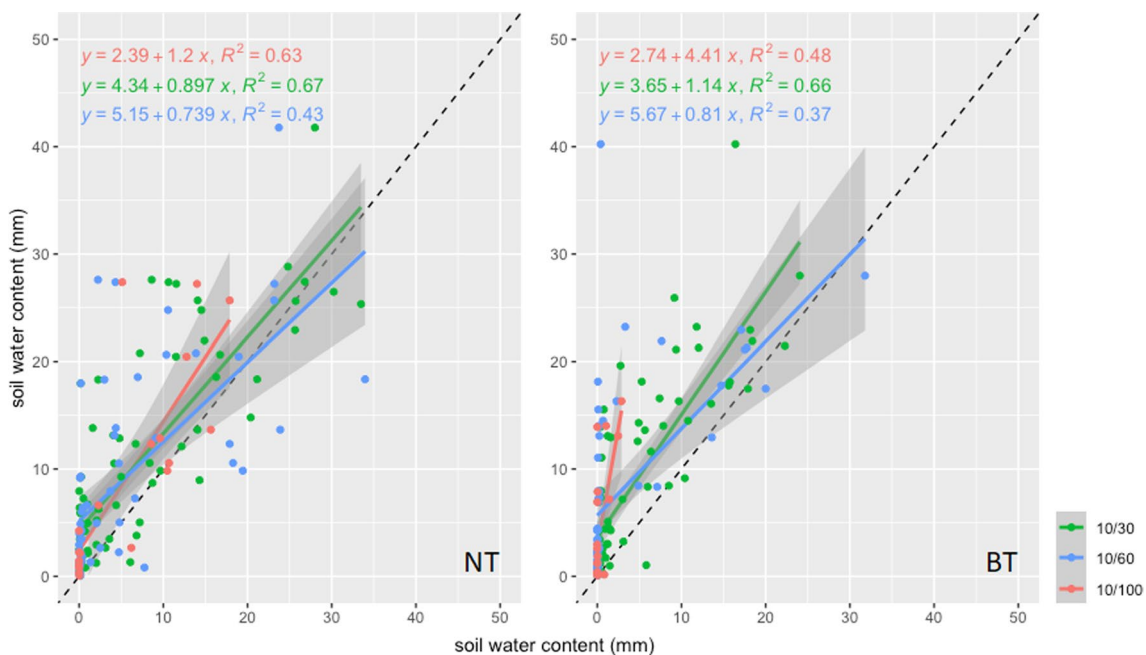


**Fig. 6**  $\Delta$ SWC probe location and stratigraphy of the soils; correlation: 10/30 cm of  $\Delta$ SWCs = green, 10/60 cm of  $\Delta$ SWCs = blue, and 10/100 cm of  $\Delta$ SWCs = red (points and lines); the gray interval repre-

sents the confidence interval at the significance level  $< 0.05$ ; dashed line is 1:1 ratio of  $\Delta$ SWC (mm) at 10 cm to other  $\Delta$ SWC (mm) at 30, 60, and 100 cm. (Color figure online)

**Acknowledgements** The authors thank the Training Forest Enterprise Masaryk Forest Křtiny for cooperation and provision of the research plots. This study was supported by the Internal Grant Schemes of Mendel University in Brno, registration no.: CZ.02.2.69/0.0/0.0/19\_073/0016670, funded by the ESF.

**Author contributions** JD, OH, and TV helped in conceptualization; JD and TV helped in methodology; JD, OH, and TV helped in validation; OH contributed to formal analysis; JD, OH, and TV worked in data analysis; MB, OH, GT, TV, and NŽ helped in investigation; MB, JD, OH, and TV contributed to writing and original draft preparation; OH and PK contributed to writing—review and editing; NŽ helped in visualization; JD and PK worked in supervision; and TV worked in project administration. All authors have read and agreed to the published version of the manuscript.

**Funding** Open access publishing supported by the National Technical Library in Prague. This study was supported by the Internal Grant Schemes of Mendel University in Brno, Registration No.: CZ.02.2.69/0.0/0.0/19\_073/0016670, funded by the ESF.

**Data availability** Data are available from the authors on request.

**Code availability** Not applicable.

## Declarations

**Conflict of interest** The authors declare no conflict of interest.

**Open Access** This article is licensed under a Creative Commons Attribution 4.0 International License, which permits use, sharing, adaptation, distribution and reproduction in any medium or format, as long as you give appropriate credit to the original author(s) and the source, provide a link to the Creative Commons licence, and indicate if changes were made. The images or other third party material in this article are included in the article's Creative Commons licence, unless indicated otherwise in a credit line to the material. If material is not included in the article's Creative Commons licence and your intended use is not permitted by statutory regulation or exceeds the permitted use, you will need to obtain permission directly from the copyright holder. To view a copy of this licence, visit <http://creativecommons.org/licenses/by/4.0/>.

## References

- Abdallah MAB, Durfee N, Mata-Gonzalez R, Ochoa CG, Noller JS (2020) water use and soil moisture relationships on western juniper trees at different growth stages. *Water* 12:1596. <https://doi.org/10.3390/w12061596>
- Agnese C, Bagarello V, Baiamonte G, Iovino M (2011) Comparing physical quality of forest and pasture soils in a Sicilian watershed. *Soil Sci Soc Am J* 75:1958–1970. <https://doi.org/10.2136/sssaj2011.0044>
- Al Hagrey SA (2007) Geophysical imaging of root-zone, trunk, and moisture heterogeneity. *J Exp Bot* 58(4):839–854. <https://doi.org/10.1093/jxb/erl237>
- Alaoui A, Caduff U, Gerke HH, Weingartner R (2011) Preferential flow effects on infiltration and runoff in grassland and Forest soils. *Vadose Zone J* 10:367–377. <https://doi.org/10.2136/vzj2010.0076>
- Bachmair S, Weiler M (2011) New dimensions of hillslope hydrology. In: Levia D, Carlyle-Moses D, Tanaka T (eds) *Forest hydrology and biogeochemistry*. Ecological studies 216. Springer, Dordrecht. [https://doi.org/10.1007/978-94-007-1363-5\\_23](https://doi.org/10.1007/978-94-007-1363-5_23)
- Banks EW, Brunner P, Simmons CT (2011) Vegetation controls on variably saturated processes between surface water and groundwater and their impact on the state of connection. *Water Resour Res*. <https://doi.org/10.1029/2011WR010544>
- Berger TW, Untersteiner H, Schume H, Jost G (2008) Throughfall fluxes in a secondary spruce (*Picea abies*), a beech (*Fagus sylvatica*) and a mixed spruce-beech stand. *For Ecol Manag* 255(3–4):605–618. <https://doi.org/10.1016/j.foreco.2007.09.030>
- Beven K, Germann P (1982) Macropores and water flow in soils. *Water Resour Res* 18(5):1311–1325. <https://doi.org/10.1029/WR018i005p01311>
- Beven K, Germann P (2013) Macropores and water flow in soils revisited. *Water Resour Res* 49(6):3071–3092. <https://doi.org/10.1002/wrcr.20156>
- Bíba M, Vícha JK, Jarabáč M (2010) Forest regeneration in experimental catchment Červík and its influence on run-off process. [Obnova lesa v experimentálním povodí Červík a její vliv na odtokový proces]. *Zprávy Lesnického Výzkumu* 2:126–132
- Bosch JM, Hewlett JD (1982) A review of catchment experiments to determine the effect of vegetation changes on water yield and evapotranspiration. *J Hydrol* 55(1–4):3–23. [https://doi.org/10.1016/0022-1694\(82\)90117-2](https://doi.org/10.1016/0022-1694(82)90117-2)
- Breshears DD, Myers OB, Barnes FJ (2009) Horizontal heterogeneity in the frequency of plant-available water with woodland intercanopy-canopy vegetation patch type rivals that occurring vertically by soil depth. *Ecohydrology* 2(4):503–519. <https://doi.org/10.1002/eco.75>
- Burt TP, Butcher DP (1985) Topographic controls of soil moisture distributions. *J Soil Sci* 36:469–486. <https://doi.org/10.1111/j.1365-2389.1985.tb00351.x>
- Carlyle-Moses DE, Iida S, Germer S, Llorens P, Michalzik B, Nanko K, Tanaka T, Tischer A, Levia DF (2020) Commentary: what we know about stemflow's infiltration area. *Front for Glob Change*. <https://doi.org/10.3389/ffgc.2020.577247>
- Černohous V, Švihla V, Šach F (2017) Contribution to assessment of forest stand impact on decrease of flood peakflow discharge. *Zprávy Lesnického Výzkumu* 62:82–86
- Chandler KR, Stevens CJ, Binley A, Keith AM (2018) Influence of tree species and forest land use on soil hydraulic conductivity and implications for surface runoff generation. *Geoderma* 310:120–127. <https://doi.org/10.1016/j.geoderma.2017.08.011>
- Chen Y, Day SD, Wick AF, Strahm BD, Wiseman PE, Daniels WL (2013) Changes in soil carbon pools and microbial biomass from urban land development and subsequent post-development soil rehabilitation. *Soil Biol Biochem* 66:38–44. <https://doi.org/10.1016/j.soilbio.2013.06.022>
- Coppola A, Kutílek M, Frind EO (2009) Transport in preferential flow domains of the soil porous system: measurement, interpretation, modelling, and upscaling. *J Contam Hydrol* 104(1–4):1–3. <https://doi.org/10.1016/j.jconhyd.2008.05.011>
- Crockford RH, Richardson DP (2000) Partitioning of rainfall into throughfall, stemflow and interception effect of forest type, ground cover and climate. *Hydrol Process* 14(16–17):2903–2920. [https://doi.org/10.1002/1099-1085\(200011/12\)14:16/17%3c2903::AID-HYP126%3e3.0.CO;2-6](https://doi.org/10.1002/1099-1085(200011/12)14:16/17%3c2903::AID-HYP126%3e3.0.CO;2-6)
- Czech Hydrometeorological Institute (2023) Available at: <https://www.chmi.cz/historicka-data/pocasi/zakladniinformace>. Accessed 1 Mar 2023
- Danjon F, Sinoquet H, Godin C, Colin F, Drexhage M (1999) Characterisation of structural tree root architecture using 3D digitising and AMAPmod software. *Plant Soil* 211(2):241–258. <https://doi.org/10.1023/A:1004680824612>
- Deutscher J, Kupec P, Dundek P, Holík L, Machala M, Urban J (2016) Diurnal dynamics of streamflow in an upland forested micro-watershed during short precipitation-free periods is altered by

- tree sap flow. *Hydrol Process* 30:2042–2049. <https://doi.org/10.1002/hyp.10771>
- Devitt DA, Smith SD (2002) Root channel macropores enhance downward movement of water in a Mojave Desert ecosystem. *J Arid Environ* 50(1):99–108. <https://doi.org/10.1006/jare.2001.0853>
- Dhiedt E, Baeten L, De Smedt P et al (2022) Tree neighbourhood-scale variation in topsoil chemistry depends on species identity effects related to litter quality. *Eur J For Res* 141:1163–1176. <https://doi.org/10.1007/s10342-022-01499-9>
- Dymond SF, Bradford JB, Bolstad PV, Kolka RK, Sebestyen SD, DeSutter TM (2017) Topographic, edaphic, and vegetative controls on plant-available water. *Ecohydrology*. <https://doi.org/10.1002/eco.1897>
- Dymond SF, Wagenbrenner JW, Keppeler ET, Bladon KD (2021) Dynamic hillslope soil moisture in a Mediterranean montane watershed. *Water Resour Res* 57:e2020WR029170. <https://doi.org/10.1029/2020WR029170>
- Eisenbies MH, Aust WM, Burger JA, Adams MB (2007) Forest operations, extreme flooding events, and considerations for hydrologic modeling in the Appalachians: a review. *For Ecol Manag* 242(2–3):77–98. <https://doi.org/10.1016/j.foreco.2007.01.051>
- Fan J, McConkey B, Wang H, Janzen H (2016) Root distribution by depth for temperate agricultural crops. *Field Crop Res* 189:68–74. <https://doi.org/10.1016/j.fcr.2016.02.013>
- Fox DM, Bryan RB, Price AG (1997) The influence of slope angle on final infiltration rate for interrill, conditions. *Geoderma* 80(1–2):181–194. [https://doi.org/10.1016/S0016-7061\(97\)00075-X](https://doi.org/10.1016/S0016-7061(97)00075-X)
- Francis CF, Thornes JB, Romero Diaz A, Lopez BF, Fisher GC (1986) Topographic control of soil moisture, vegetation cover and land degradation in a moisture stressed Mediterranean environment. *CATENA* 13:211–225. [https://doi.org/10.1016/S0341-8162\(86\)80014-5](https://doi.org/10.1016/S0341-8162(86)80014-5)
- Frischbier N, Tiesel K, Tischer A, Wagner S (2019) Small scale rainfall partitioning in a European beech forest ecosystem reveals heterogeneity of leaf area index and its connectivity to hydro- and atmosphere. *Geosciences* 9:393. <https://doi.org/10.3390/geosciences9090393>
- Ganatsios HP, Tsioras PA, Pavlidis T (2010) Water yield changes as a result of silvicultural treatments in an oak ecosystem. *For Ecol Manag* 260(8):1367–1374. <https://doi.org/10.1016/j.foreco.2010.07.033>
- Germer S et al (2012) Pan-European beech (*Fagus sylvatica*) stemflow data comparison. *Geophys Res Abstr* 14 (EGU2012–12761)
- Ghestem M, Sidle RC, Stokes A (2011) The influence of plant root systems on subsurface flow: implications for slope stability. *Bioscience* 61(11):869–879. <https://doi.org/10.1525/bio.2011.61.11.6>
- Greiffenhagen A, Wessolek G, Facklam M, Renger M, Stoffregen H (2006) Hydraulic functions and water repellency of forest floor horizons on sandy soils. *Geoderma* 132:182–195. <https://doi.org/10.1016/j.geoderma.2005.05.006>
- Guo FX, Wang YP, Hou TT, Zhang LS, Mu Y, Wu FY (2021) Variation of soil moisture and fine roots distribution adopts rainwater collection, infiltration promoting and soil anti-seepage system (RCIP-SA) in hilly apple orchard on the Loess Plateau of China. *Agric Water Manag* 244:106573
- Herwitz SR (1986) Infiltration-excess caused by stemflow in a cyclone-prone tropical rainforest. *Earth Surf Proc Land* 11(4):401–412. <https://doi.org/10.1002/esp.3290110406>
- Hirte J, Leifeld J, Abiven S, Mayer J (2018) Maize and wheat root biomass, vertical distribution, and size class as affected by fertilization intensity in two long-term field trials. *Field Crop Res* 216:197–208. <https://doi.org/10.1016/j.fcr.2017.11.023>
- Hrachowitz M, Savenije HHG, Blöschl G et al (2013) A decade of predictions in ungauged basins (PUB)—a review. *Hydrol Sci J* 58(6):1198–1255. <https://doi.org/10.1080/02626667.2013.803183>
- Jačka L, Walmsley A, Kovář M, Frouz J (2021) Effects of different tree species on infiltration and preferential flow in soils developing at a clayey spoil heap. *Geoderma*. <https://doi.org/10.1016/j.geoderma.2021.115372>
- Jačka L, Valtera M, Juras R, Deutscher J, Hemr O, Pavlásek J, (2020) The effect of microrelief on preferential flow and subsurface runoff in forest soils: a study using rain simulator and dye tracer. *Contemplating earth: soil and landscape considerations (conference proceedings)* Brno. Mendel University in Brno. ISBN 978-80-7509-766-8
- Jarvis NJ (2007) A review of non-equilibrium water flow and solute transport in soil macropores: Principles, controlling factors and consequences for water quality. *Eur J Soil Sci* 58(3):523–546. <https://doi.org/10.1111/j.1365-2389.2007.00915.x>
- Jochheim H, Lüttschwager D, Riek W (2002) Stem distance as an explanatory variable for the spatial distribution and chemical conditions of stand precipitation and soil solution under beech (*Fagus sylvatica* L.) trees. *J Hydrol*. <https://doi.org/10.1016/j.jhydrol.2022.127629>
- Johnson S, Lehmann J (2006) Stemflow and root-induced preferential flow: the double-funneling of trees. *Ecoscience* 13:324–333. <https://doi.org/10.2980/i1195-6860-13-3-324.1>
- Jones A (1971) Soil piping and stream channel initiation. *Water Resour Res* 7(3):602–610. <https://doi.org/10.1029/WR007i003p00602>
- Jordán A, Martínez-Zavala L, Bellinfante N (2008) Heterogeneity in soil hydrological response from different land cover types in southern Spain. *CATENA* 74:137–143. <https://doi.org/10.1016/j.catena.2008.03.015>
- Julich S, Kreiselmeier J, Scheibler S, Petzold R, Schwärzel K, Feger KH (2021) Hydraulic properties of forest soils with stagnic conditions. *Forests* 12:1113. <https://doi.org/10.3390/f12081113>
- Juříčka D, Valtera M, Deutscher J, Vichta T, Pecina V, Patočka Z, Chalupová N, Tomášová G, Jačka L, Pařílková J (2022) The role of pit-mound microrelief in the redistribution of rainwater in forest soils: a natural legacy facilitating groundwater recharge? *Eur J for Res* 141:321–345. <https://doi.org/10.1007/s10342-022-01439-7>
- Koestel JK, Moeys J, Jarvis NJ (2012) Meta-analysis of the effects of soil properties, site factors and experimental conditions on solute transport. *Hydrol Earth Syst Sci* 16(6):1647–1665. <https://doi.org/10.5194/hess-16-1647-2012>
- Kuentz A, Arheimer B, Hundecha Y, Wagener T (2017) Understanding hydrologic variability across Europe through catchment classification. *Hydrol Earth Syst Sci* 21:2863–2879. <https://doi.org/10.5194/hess-21-2863-2017>
- Kučec P, Deutscher J, Školoud L (2019) Water use efficiency of forested upland micro-watersheds as affected by the dominant tree species composition. [Vodohospodářská účinnost zalesněných pahorkatinných mikropovodí s rozdílnou hlavní dřevinou v bezesrážkových periodách]. *Zprávy Lesnického Výzkumu* 64(2):86–93
- Lal R, Shukla MK (2004) Principles of soil physics. Marcel Dekker Inc, New York
- Levia DF, Hudson SA, Llorens P, Nanko K (2017) Throughfall drop size distributions: a review and prospectus for future research. *Wiley Interdiscip Rev: Water*. <https://doi.org/10.1002/WAT2.1225>
- Levia DF, Keim RF, Carlyle-Moses DE, Frost EE (2011) In: Levia, D., Carlyle-Moses, D., Tanaka, T. (eds) *Forest hydrology and biogeochemistry*. Ecological studies 216. Springer, Dordrecht. [https://doi.org/10.1007/978-94-007-1363-5\\_23](https://doi.org/10.1007/978-94-007-1363-5_23)
- Liang WL, Kosugi KI, Mizuyama T (2011) Soil water dynamics around a tree on a hillslope with or without rainwater supplied by stemflow. *Water Resour Res*. <https://doi.org/10.3390/f14030507>
- Liu H, Lei TW, Zhao J, Yuan CP, Fan YT, Qu LQ (2011) Effects of rainfall intensity and antecedent soil water content on soil infiltrability under rainfall conditions using the run off-on-out

- method. *J Hydrol* 396(1–2):24–32. <https://doi.org/10.1016/j.jhydrol.2010.10.028>
- Liu Z, Wang Y, Xu Z, Duan Q (2019) Conceptual hydrological models. In: Handbook of hydrometeorological ensemble forecasting. Springer, Berlin, Heidelberg, pp 389–411. [https://doi.org/10.1007/978-3-642-39925-1\\_22](https://doi.org/10.1007/978-3-642-39925-1_22)
- Llorens P, Latron J, Carlyle-Moses DE, Näthe K, Chang JL, Nanko K, Iida S, Levia DF (2022) Stemflow infiltration areas into forest soils around American beech (*Fagus grandifolia* Ehrh.) trees. *Ecology* 15(2):e2369. <https://doi.org/10.1002/eco.2369>
- Malik I, Pawlik Ł, Slezak A, Wistuba M (2019) A study of the wood anatomy of *Picea abies* roots and their role in biomechanical weathering of rock cracks. *CATENA* 173:264–275. <https://doi.org/10.1016/j.catena.2018.10.018>
- McGlynn BL, McDonnell JJ, Brammer DD (2002) A review of the evolving perceptual model of hillslope flowpaths at the Maimai catchments, New Zealand. *J Hydrol* 257(1–4):1–26. [https://doi.org/10.1016/S0022-1694\(01\)00559-5](https://doi.org/10.1016/S0022-1694(01)00559-5)
- McMillan H (2020) Linking hydrologic signatures to hydrologic processes: a review. *Hydrol Process* 34(6):1393–1409. <https://doi.org/10.1002/hyp.13632>
- Meesenburg H, Eichhorn J, Meiwes KJ (2009) Atmospheric deposition and canopy interactions. In: Brumme R, Khanna PK (eds) Functioning and management of European beech ecosystems. Springer, Berlin Heidelberg, pp 265–302. [https://doi.org/10.1007/b82392\\_16](https://doi.org/10.1007/b82392_16)
- Metzger JC, Filipzik J, Michalzik B, Hildebrandt A (2021) Stemflow infiltration hotspots create soil microsites near tree stems in an unmanaged mixed beech forest. *Front for Glob Change*. <https://doi.org/10.3389/fgc.2021.701293>
- Mitchell AR, Ellsworth TR, Meek BD (1995) Effect of root systems on preferential flow in swelling soil. *Commun Soil Sci Plant Anal* 26(15–16):2655–2666. <https://doi.org/10.1080/00103629509369475>
- Mosley MP (1979) Streamflow generation in a forested watershed, New Zealand. *Water Resour Res* 15(4):795–806. <https://doi.org/10.1029/WR015i004p00795>
- Mosley MP (1982) Subsurface flow velocities through selected forest soils, south island, New Zealand. *J Hydrol* 55(1–4):65–92. [https://doi.org/10.1016/0022-1694\(82\)90121-4](https://doi.org/10.1016/0022-1694(82)90121-4)
- Novosadová K, Kadlec J, Řehořková Š, Matoušková M, Urban J, Pokorný R (2023) Comparison of rainfall partitioning and estimation of the utilisation of available water in a monoculture beech forest and a mixed beech-oak-linden forest. *Water (Switzerland)*. <https://doi.org/10.3390/w15020285>
- Nyberg L (1996) Spatial variability of soil water content in the covered catchment at Gardsjon, Sweden. *Hydrol Process* 10:89–103
- Patric JH (1978) Harvesting effects on soil and water in the eastern hardwood forest. *South J Appl For* 2:66–73
- Perkons U, Kautz T, Uteau D, Peth S, Geier V, Thomas K, Lütke Holz K, Athmann M, Pude R, Köpke U (2014) Root-length densities of various annual crops following crops with contrasting root systems. *Soil Tillage Res* 137:50–57
- Pitkänen J, Nuutinen V (1998) Earthworm contribution to infiltration and surface runoff after 15 years of different soil management. *Appl Soil Ecol* 9(1–3):411–415. [https://doi.org/10.1016/S0929-1393\(98\)00098-5](https://doi.org/10.1016/S0929-1393(98)00098-5)
- Pohl M, Stroude R, Buttler A, Rixen C (2011) Functional traits and root morphology of alpine plants. *Ann Bot* 108:537–545
- Pressland AJ (1976) Soil moisture redistribution as affected by throughfall and stemflow in an arid zone shrub community. *Aust J Bot* 24(5):641–649. <https://doi.org/10.1071/BT9760641>
- R Core Team. R: A language and environment for statistical computing; R foundation for statistical computing: Vienna, Austria, 2017; <http://www.R-project.org/>. Accessed 1 Dec 2022
- Ray G, Ochoa CG, Deboodt T, Mata-Gonzalez R (2019) Overstory-understory vegetation cover and soil water content observations in western juniper woodlands: a paired watershed study in central Oregon, USA. *Forests* 10:151. <https://doi.org/10.3390/f10020151>
- Revell N, Lashford C, Rubinato M, Blackett M (2022) The impact of tree planting on infiltration dependent on tree proximity and maturity at a clay site in Warwickshire. *England Water* 14:892. <https://doi.org/10.3390/w14060892>
- Rita A, Bonanomi G, Allevato E et al (2021) Topography modulates near-ground microclimate in the Mediterranean *Fagus sylvatica* treeline. *Sci Rep* 11:8122. <https://doi.org/10.1038/s41598-021-87661-6>
- Robinson DA, Jones SB, Wraith JM, Or D, Friedman SP (2003) A review of advances in dielectric and electrical conductivity measurement in soils using time domain reflectometry. *Vadose Zone J* 2(4):444–475. <https://doi.org/10.2113/2.4.444>
- Robinson DA, Campbell CS, Hopmans JW, Hornbuckle BK, Jones SB, Knight R, Wendroth O (2008) Soil moisture measurement for ecological and hydrological watershed-scale observatories: a review. *Vadose Zone J* 7(1):358–389. <https://doi.org/10.2136/vzj2007.0143>
- Šamonil P, Král K, Hort L (2010) The role of tree uprooting in soil formation: a critical literature review. *Geoderma* 157(3–4):65–79. <https://doi.org/10.1016/j.geoderma.2010.03.018>
- Schwärzel K, Ebermann S, Schalling N (2012) Evidence of double-funneling effect of beech trees by visualization of flow pathways using dye tracer. *J Hydrol* 470:184–192. <https://doi.org/10.1016/j.jhydrol.2012.08.048>
- Sidle RC, Noguchi S, Tsuboyama Y, Laursen K (2001) A conceptual model of preferential flow systems in forested hillslopes: evidence of self-organization. *Hydrol Process* 15:1675–1692. <https://doi.org/10.1002/hyp.233>
- Spencer SA, van Meerveld HJ (2016) Double funnelling in a mature coastal British Columbia forest: spatial patterns of stemflow after infiltration. *Hydrol Process* 30(22):4185–4201. <https://doi.org/10.1002/hyp.10936>
- Staelens J, De Schrijver A, Verheyen K, Verhoest NEC (2006) Spatial variability and temporal stability of throughfall water under a dominant beech (*Fagus sylvatica* L.) tree in relationship to canopy cover. *J Hydrol* 330(3–4):651–662. <https://doi.org/10.1016/j.jhydrol.2006.04.032>
- Staelens J, De Schrijver A, Verheyen K, Verhoest NEC (2008) Rainfall partitioning into throughfall, stemflow, and interception within a single beech (*Fagus sylvatica* L.) canopy: influence of foliation, rain event characteristics, and meteorology. *Hydrol Process* 22(1):33–45. <https://doi.org/10.1002/hyp.6610>
- Van Stan JT, Gutmann E, Friesen, J (2020) Precipitation partitioning by vegetation: a global synthesis. *Precipitation partitioning by vegetation: a global synthesis*. <https://doi.org/10.1007/978-3-030-29702-2>
- Švihla V, Šach F, Černošou V (2016) Influence of clearcuttings or impact of rapid broad disintegration of a forest on total run-off by growing seasons. [Vliv holých sečí či rychlého vepoklošného rozpadu lesa na celkový odtok za vegetační období]. *Zprávy Lesnického Výzkumu* 61(2):138–144
- Taniguchi M, Tsujimura M, Tanaka T (1996) Significance of stemflow in groundwater recharge I: evaluation of the stemflow contribution to recharge using a mass balance approach. *Hydrol Process* 10(1):71–80. [https://doi.org/10.1002/\(SICI\)1099-1085\(199601\)10:1%3c71::AID-HYP301%3e3.0.CO;2-Q](https://doi.org/10.1002/(SICI)1099-1085(199601)10:1%3c71::AID-HYP301%3e3.0.CO;2-Q)
- Tomlin AD, Shipitalo MJ, Edwards WM, Protz R (1995) Earthworms and their influence on soil structure and infiltration. In: Press, CRC (ed) Earthworm ecology and biogeography in North America. Boca Raton, pp 159–184

- Troch PA, Martinez GF, Pauwels VRN, Durcik M, Sivapalan M, Harman C, Huxman T (2009) Climate and vegetation water use efficiency at catchment scales. *Hydrol Process* 23(16):2409–2414. <https://doi.org/10.1002/hyp.7358>
- Tromp-Van Meerveld HJ, McDonnell JJ (2006) Threshold relations in subsurface stormflow: 2. the fill and spill hypothesis. *Water Resour Res*. <https://doi.org/10.1029/2004WR003800>
- Uchida T, Kosugi K, Mizuyama T (2001) Effects of pipeflow on hydrological process and its relation to landslide: a review of pipeflow studies in forested headwater catchments. *Hydrol Process* 15(11):2151–2174. <https://doi.org/10.1002/hyp.281>
- Valtera M, Schatzl RJ (2017) Pit-mound microrelief in forest soils: review of implications for water retention and hydrologic modelling. *For Ecol Manag* 393:40–51. <https://doi.org/10.1016/j.foreco.2017.02.048>
- Van Stan JT, Allen ST (2020) What we know about stemflow's infiltration area. *Front for Glob Change* 3:61. <https://doi.org/10.3389/ffgc.2020.00061>
- Vereecken H, Huisman JA, Bogen H, Vanderborght J, Vrugt JA, Hopmans JW (2008) On the value of soil moisture measurements in vadose zone hydrology: a review. *Water Resour Res*. <https://doi.org/10.1029/2008WR006829>
- Wahren A, Schwärzel K, Feger K (2012) Potentials and limitations of natural flood retention by forested land in headwater catchments: evidence from experimental and model studies. *J Flood Risk Manag* 5(4):321–335. <https://doi.org/10.1111/j.1753-318X.2012.01152.x>
- Wang XP, Cui Y, Pan YX, Li XR, Yu Z, Young MH (2008) Effects of rainfall characteristics on infiltration and redistribution patterns in revegetation-stabilized desert ecosystems. *J Hydrol* 358(1–2):134–143
- Wang S, Fu B, Gao G, Liu Y, Zhou J (2013) Responses of soil moisture in different land cover types to rainfall events in a re-vegetation catchment area of the Loess Plateau, China. *CATENA* 101:122–128. <https://doi.org/10.1016/j.catena.2012.10.006>
- Weiler M (2017) Macropores and preferential flow: a love-hate relationship. *Hydrol Process* 31(1):15–19. <https://doi.org/10.1002/hyp.11074>
- Weiss A. Topographic position and landforms analysis 2001, In: Poster presentation, ESRI user conference, Vol. 561 200, San Diego
- Wessolek G, Schwärzel K, Greiffenhagen A, Stoffregen H (2008) Percolation characteristics of a water-repellent sandy forest soil. *Eur J Soil Sci* 59(1):14–23. <https://doi.org/10.1111/j.1365-2389.2007.00980.x>
- Wickham H (2016) *ggplot2: elegant graphics for data analysis*. Springer-Verlag, New York, p 2016
- Wild J, Kopecký M, Macek M, Šanda M, Jankovec J, Haase T (2019) Climate at ecologically relevant scales: a new temperature and soil moisture logger for long-term microclimate measurement. *Agric for Meteorol* 268:40–47. <https://doi.org/10.1016/j.agrformet.2018.12.018>
- Zhang D, Wang Z, Guo Q, Lian J, Chen L (2019) Increase and spatial variation in soil infiltration rates associated with fibrous and tap tree roots. *Water* 11:1700. <https://doi.org/10.3390/w11081700>
- Zimmermann B, Elsenbeer H, De Moraes JM (2006) The influence of land-use changes on soil hydraulic properties: implications for runoff generation. *For Ecol Manag* 222:29–38. <https://doi.org/10.1016/j.foreco.2005.10.070>

**Publisher's Note** Springer Nature remains neutral with regard to jurisdictional claims in published maps and institutional affiliations.